

## Dissolution and Release Behavior of Hydrogen Isotopes from Barium-Zirconates

M. Khalid Hossain

Department of Advanced Energy Engineering Science, Interdisciplinary Graduate School of Engineering Science, Kyushu University

Hashizume, Kenichi

Department of Advanced Energy Engineering Science, Interdisciplinary Graduate School of Engineering Science, Kyushu University

<https://doi.org/10.5109/4102460>

---

出版情報 : Proceedings of International Exchange and Innovation Conference on Engineering & Sciences (IEICES). 6, pp.34-39, 2020-10-22. Interdisciplinary Graduate School of Engineering Sciences, Kyushu University

バージョン :

権利関係 :



# Dissolution and Release Behavior of Hydrogen Isotopes from Barium-Zirconates

\*M. Khalid Hossain<sup>1,2</sup>, Kenichi Hashizume<sup>1</sup>

<sup>1</sup>Department of Advanced Energy Engineering Science, Interdisciplinary Graduate School of Engineering Science, Kyushu University, Kasuga, Fukuoka 816-8580, Japan,

<sup>2</sup>Atomic Energy Research Establishment, Bangladesh Atomic Energy Commission, Dhaka 1349, Bangladesh.

\*Corresponding author email: khalid.baec@gmail.com, khalid@kyudai.jp

**ABSTRACT:** Hydrogen release behavior from perovskite proton conducting oxide, yttrium doped barium-zirconate,  $BaZr_{0.9}Y_{0.1}O_{3-\alpha}$  (BZY) exposed to  $D_2$  or  $D_2O$  atmosphere was studied by thermal desorption spectroscopy (TDS) detecting deuterium gas ( $D_2$ ) and heavy water vapor ( $D_2O$ ) separately. The release of hydrogen appeared at around 950-1175 K. Hydrogen solubility was higher in the BZY sample exposed to the  $D_2O$ .

**Keywords:** Barium-zirconate, perovskite oxide, hydrogen dissolution, hydrogen solubility, TDS.

## 1. INTRODUCTION

Perovskite oxides-based proton and electronics conducting ceramic membrane has drawn considerable attention for hydrogen separation applications over the last few decades due to several advantages like thermal stability, good mechanical strength, high hydrogen permeation flux, and chemical resistivity in corrosive environments [1,2]. The extensively studied Pd-based membranes showed poor stability and high cost of Pd, whereas conventional membranes of proton conducting materials exhibit much lower hydrogen permeation. Comparing all proton-conducting oxides, as the temperature increased  $BaCeO_3$  based perovskite shows the highest conductivity with the contribution of ionic conduction of oxygen [3]. The improvement of perovskite oxides membrane proton conducting properties is essential to consider trivalent rare-earth atom at B-site. Tan et al. (2012) [4] focused on Tb-doped  $BaCeO_3$  ( $BaCe_{0.95}Tb_{0.05}O_{3-\alpha}$ ) based perovskite oxides having higher proton conductivity but lower electronic conductivity. The effective way of promoting hydrogen permeation flux is to reduce membrane thickness and the sintering process of the membrane. Throughout the last few decades: the ceramic membranes of hollow fiber geometry have been used to design and develop with the inclusion of combined phase inversion and sintering technique, because of high-temperature scaling, thin effective membrane thickness and larger membrane area as per unit packing volume. The rate of high hydrogen production is possible to achieve using a hollow fiber membrane module at large specific membrane areas irrespective of the lower permeability of the individual membrane.

Low-level tritium detection is an imperative issue in tritium handling facilities due to their potential radioactive properties. In recent times, the development and utilization of various tritium monitors to control the radiation have been reported [5]. In addition, to improve the performance of the tritium monitor in terms of low concentration tritium detection, the implication of hydrogen pump as a membrane separator which consists of proton conducting oxide has been proposed by Tanaka et al. (2008) (Fig. 1) [6]. The research group used  $CaZr_{0.9}In_{0.1}O_{3-\alpha}$  as proton conducting oxide to recover the low concentration tritium [7]. In the next comprehensive study, the tritium monitor's technical

feasibility was investigated by the integration test of the system consisting of a proportional counter combined with an electrochemical hydrogen pump [8].

As proton-conducting oxides are promising materials for electrochemical devices like fuel cell, hydrogen pump, hydrogen sensor, and for nuclear fusion reactor's tritium purification [9–14], recovery [10,15–19], and monitoring system, therefore, the study of hydrogen behavior in such oxide materials is very fundamental and important. Yttrium (Y) doped barium-zirconate ( $BaZrO_3$ ) is a proton-conducting oxide that has a perovskite structure [20]. In this study, the dissolution of hydrogen in BZYC specimens was done using  $D_2$  gas and  $D_2O$  vapor

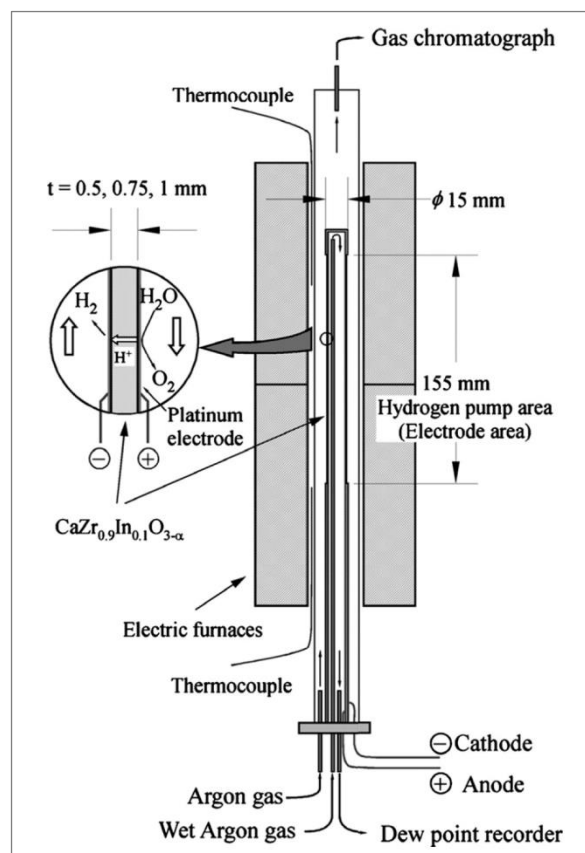


Fig. 1. Schematic of the hydrogen pump apparatus consists with proton-conducting oxide for the tritium monitoring. Reproduce with permission from Ref. [6].

separately. Then the hydrogen release and hydrogen solubility were investigated by the thermal desorption spectroscopy (TDS) method.

## 2. EXPERIMENTAL

### 2.1 Sample preparation

The disc shape specimen (diameter: 7.7 mm, thickness: 2.2 mm) was prepared using a conventional powder sintering method at 1923 K for 20h, which is described elsewhere [16,21–23]. The SEM and EDX mapping

were performed before and after polishing the sample to understand its surface properties. All chemical components of the specimen were uniformly distributed throughout the surface after polishing. The sintered disc specimen was cut using a diamond saw into parallelepiped pieces ( $7.7 \times 2.2 \times 0.5 \text{ mm}^3$ ) for  $\text{D}_2$  gas or  $\text{D}_2\text{O}$  vapor exposure and TDS study.

### 2.2 $\text{D}_2$ and $\text{D}_2\text{O}$ exposure

The cut sample was placed in a quartz glass tube and evacuated to low pressure ( $\sim 10^{-6} \text{ Pa}$ ). At a temperature of

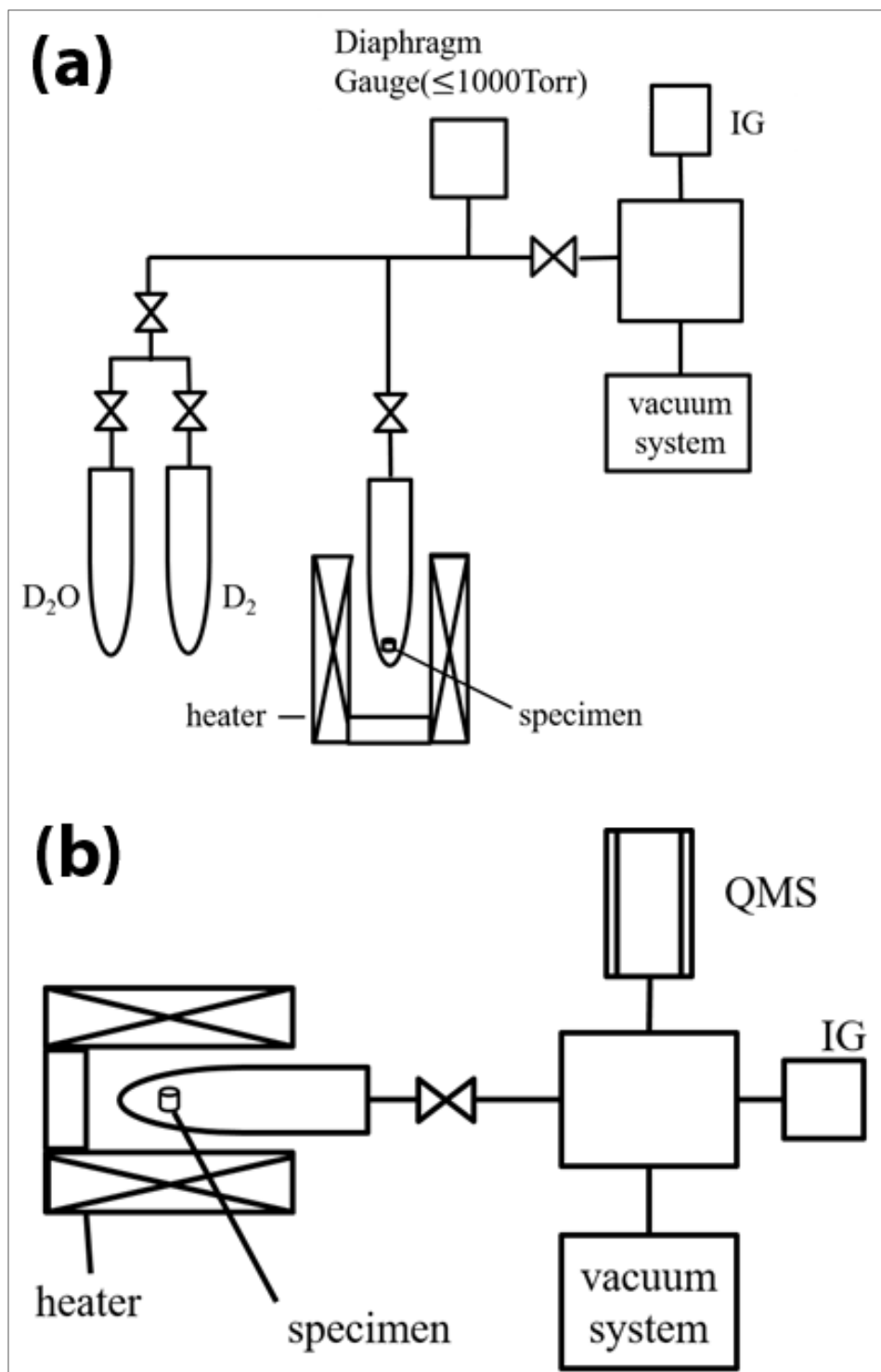


Fig. 2. (a) Schematic of  $\text{D}_2$  gas and  $\text{D}_2\text{O}$  vapor exposure apparatus, (b) schematic of temperature programmed desorption (TDS) system.

1273 K, vacuum annealing was performed for 30 min to remove the sample's volatile substances. Then at 873 K, deuterium gas ( $D_2$ , 1.3 kPa) was exposed to the sample for 1 h using the apparatus shown in Fig. 2(a) [21]. After the exposure, the quartz glass tube was quenched with room temperature water. Finally, the sample was taken out from the quartz glass tube after recovering the  $D_2$  gas. The same sample was used repeatedly for heavy water vapor ( $D_2O$ , 1.3 kPa) exposure and the TDS study.

### 2.3 $D_2$ and $D_2O$ measurement

The TDS apparatus used in this experiment to measure the released hydrogen ( $D_2$ , HD,  $D_2O$  and HDO) from the  $D_2$  gas and  $D_2O$  vapor exposed sample is shown in Fig. 2(b) [2]. First, the quartz glass tube baking without the sample was performed with an electric furnace to release and remove substances accumulated in the device at 1273 K for 30 min. After cooling down the glass tube to room temperature, the  $D_2$  gas exposed sample was placed in the TDS study's glass tube. Then after evacuating the glass

sample was allowed to raise (at a heating rate of 0.5 K/s) up to 1273 K. After 30 min stays at 1273 K, the heater power was disconnected automatically by using a programable temperature controller. The gas released from the samples was measured using a quadrupole mass spectrometer (Q-MAS) (TSPTT200, INFICON) [24] during this sample heating and cooling down cycle. The above same procedure was also applied for the  $D_2O$  exposed sample.

### 2.4 QMAS data conversion using He-standard leak

The mass spectrometer is one of the most popular instrumental analyzers that ionizes and separates chemical substances such as atoms and molecules, and finally measures the generated ions by their mass. The major parts of a mass spectrometer are the ionization part (ion source), mass analysis part (analyzer), detection part (detector), vacuum exhaust part (vacuum pump), device control part, data processing part (data system), etc. There are various types of analyzers, one of which is a

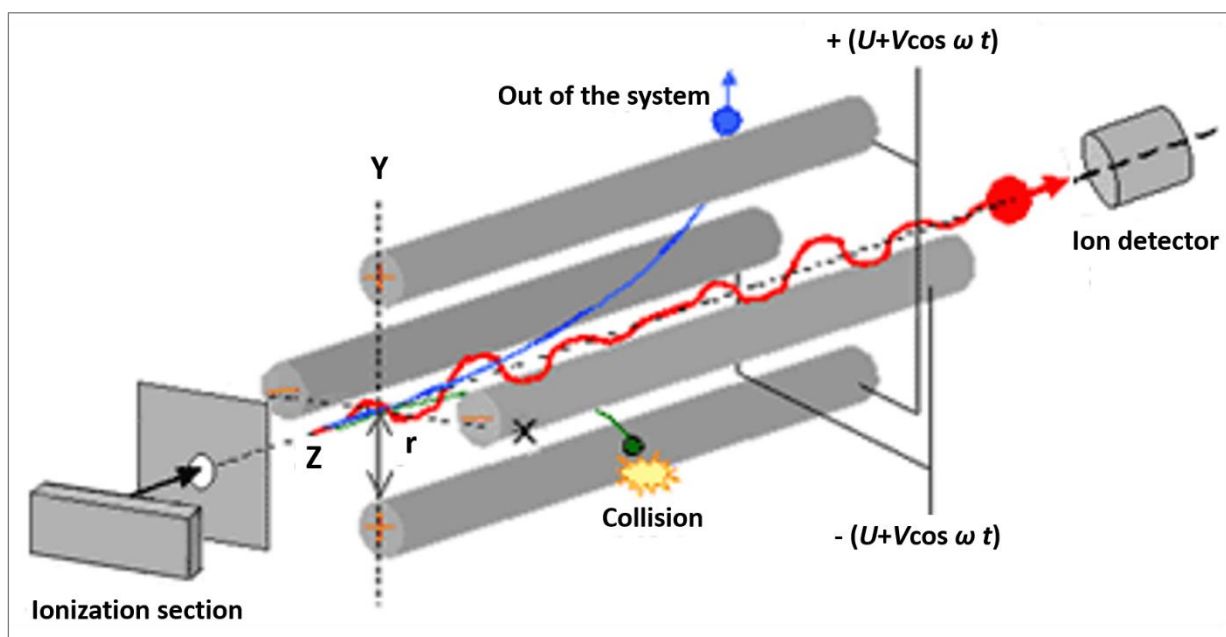


Fig. 3. Conceptual diagram of ion separation and detection in a quadrupole analyzer.



Fig. 4. Figure 13 He standard leak (Vacuum Technology Inc., Model: CL-6-He-4FVCR-500DOT-MFV).

tube to low pressure ( $\sim 10^{-6}$  Pa), the temperature of the

quadrupole, and a mass spectrometer having a

quadrupole analyzer is known as quadrupole mass spectrometer (QMAS). The features of QMS are: 1. low vacuum (usually  $\sim 10^{-5}$  Torr), 2. miniaturization, 3. high-speed scanning (latest is  $10000u/\text{sec}$  or more,  $u$  = unified atomic mass unit), 4. cheap, 5. easy to operate, 6. robust, and easy to maintain, and many other advantages.

A QMAS consists of four parallel rod-shaped electrodes (**Fig. 3**) where a superposition of DC voltage and high-frequency AC voltage,  $\pm(U+V\cos \omega t)$  is applied in the opposite electrodes having the same polarity and forms a quadrupole electric field (where  $U$  is the DC voltage,  $V$  is the maximum value of the AC voltage,  $\omega = 2\pi\nu$ ,  $\nu$  is the high frequency). In mass spectrometry, gas molecules are ionized under a high vacuum, and the generated ions are separated and analyzed in the order of

charge. When ions enter the quadrupole electrode, they are affected by the high-frequency electric field and travel in the  $z$  direction while oscillating in the  $x$  or  $y$  direction (**Fig. 3**). But only ions with a specific  $m/z$  value make stable oscillatory motion, pass through the quadrupole, and reach the detector. On the other hand, ions with other  $m/z$  values have large amplitude and diverge and collide with the electrode. When the frequency  $f$  is constant and  $U/V$  have a certain value, only ions satisfying  $m/z = 0.14 V/f^2 r^2$ . Therefore, if  $V$  is continuously changed while  $U/V$  is kept constant, ions corresponding to each mass will be separated and

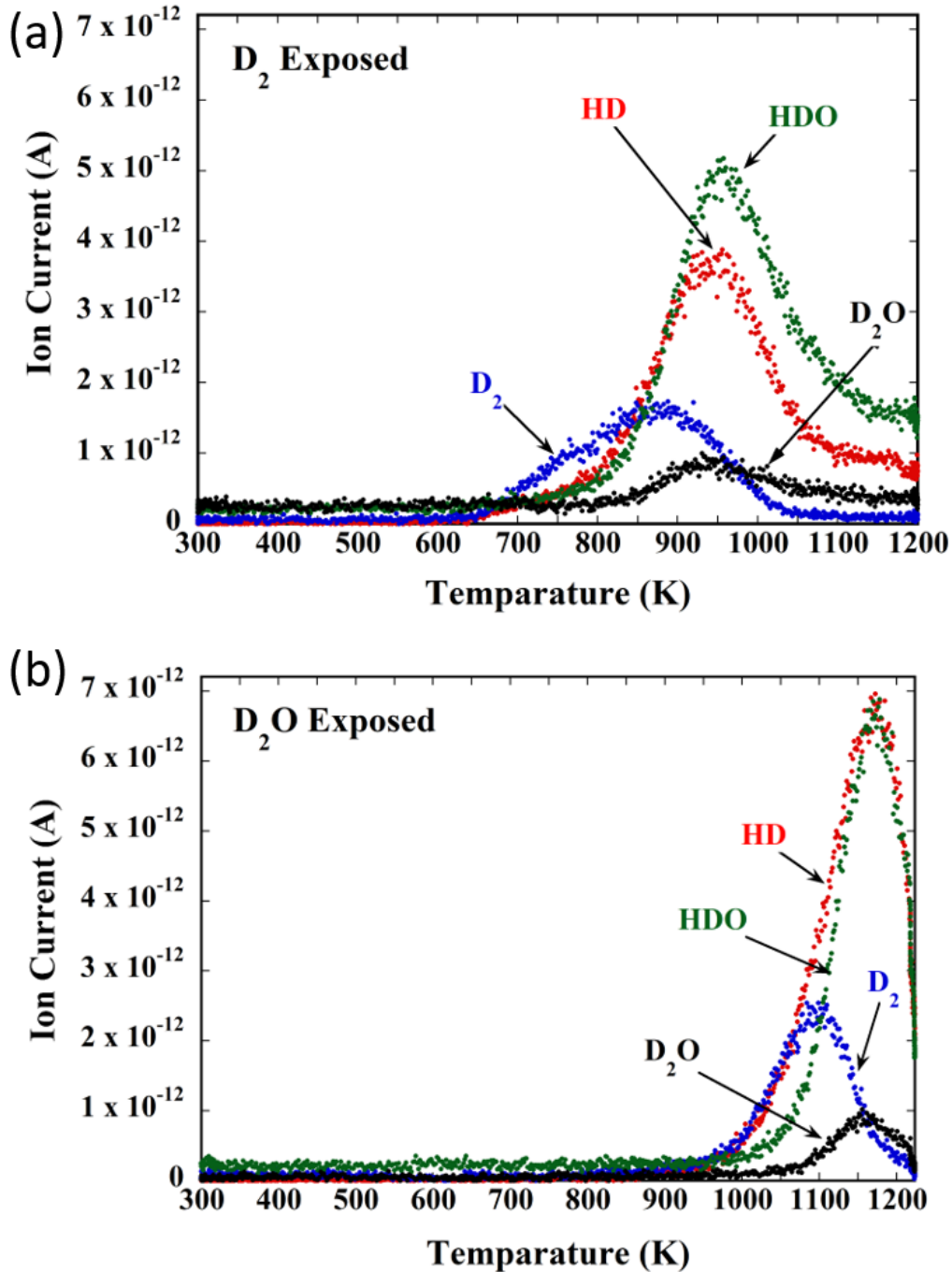


Fig. 5. TDS results for (a) D<sub>2</sub> gas, and (b) D<sub>2</sub>O vapor exposure samples.

the magnitude of the ratio  $m/z$ , where  $m$  = mass, and  $z$  =



Table 1. D amount released from D<sub>2</sub> and D<sub>2</sub>O exposed samples.

Deuterium (D) amount	D <sub>2</sub> exposed sample	D <sub>2</sub> O exposed sample
D from D <sub>2</sub> and HD (D/M)	5.5 x 10 <sup>-5</sup>	1.4 x 10 <sup>-3</sup>
D from D <sub>2</sub> O and HDO (D/M)	7.5 x 10 <sup>-5</sup>	1.1 x 10 <sup>-3</sup>
Total D (D/M)	1.3 x 10 <sup>-4</sup>	2.5 x 10 <sup>-3</sup>
Fraction of deuterium gas (%)	42	56
Fraction of water vapor (%)	58	44

detected. The passing ion stream is usually detected by an electron amplifier tube. In the electron amplifier tube, a small number of incident ions hit the metal surface and emit a large number of secondary electrons. By repeating this, secondary electrons are multiplied, and a small number of ions can be detected with high sensitivity.

A standard He leak experiment was carried out to convert the measured current value obtained from Q-MAS data into the amount of emission. The leaked amount of He standard leak (Company name: Vacuum Technology Inc., Model: CL-6-He-4FVCR-500DOT-MFV, Serial: D15543 (Fig. 4)) used in the experiment was  $1.8 \times 10^{-7}$  (Pa · m<sup>3</sup> / s). Since the inside of the apparatus is evacuated, it is assumed that the state is close to an ideal gas. In that case, from the equation of state of the gas,

$$n = \frac{PV}{RT} = \frac{1.8 \times 10^{-7}}{8.31 \times 297} \left[ \frac{\text{Pa m}^3 \text{ s}^{-1}}{\text{J K}^{-1} \text{ mol}^{-1} \text{ K}} \right] = 7.46 \times 10^{-11} [\text{mol/s}] \quad (8)$$

The leak rate (n) of the He standard leak is  $7.46 \times 10^{-11}$  [mol/s].

### 3. RESULTS AND DISCUSSION

The ion currents obtained from Q-MAS data for the D<sub>2</sub> gas and D<sub>2</sub>O vapor exposed samples are shown in Fig. 5. In the case of D<sub>2</sub> exposed sample HD, HDO, and D<sub>2</sub>O was released at 950 K whereas D<sub>2</sub> released at 875 K. In the case of D<sub>2</sub>O exposed sample HD, and HDO was released at 1175 K whereas D<sub>2</sub> and D<sub>2</sub>O were released at 1150 K and 1100 K, respectively. The highest release peak was detected as HDO gas from D<sub>2</sub> exposed sample and there may appear a trend for the hydrogen release as HDO > HD > D<sub>2</sub> > D<sub>2</sub>O. On the other hand, the highest peak was observed as HD and HDO vapor from D<sub>2</sub>O exposed sample and there may appear a trend for the hydrogen release as HD = HDO > D<sub>2</sub> > D<sub>2</sub>O.

The total amounts of D-containing gas released from the D<sub>2</sub> or D<sub>2</sub>O exposed samples and its ratios are listed in Table 1. The total amount of deuterium (D) released from D<sub>2</sub> exposed sample was  $1.3 \times 10^{-4}$  (D/M), where released deuterium gas and water vapor were  $\sim 5.5 \times 10^{-5}$  (D/M) and  $\sim 7.5 \times 10^{-5}$  (D/M), respectively. On the other hand, the total amount of D released from D<sub>2</sub>O exposed sample was  $2.5 \times 10^{-3}$  (D/M), where released deuterium gas and water vapor were  $\sim 1.4 \times 10^{-3}$  (D/M) and  $\sim 1.1 \times 10^{-3}$  (D/M), respectively. The percentage of water vapor released from the D<sub>2</sub> exposed sample is higher than that of the D<sub>2</sub>O exposed sample, whereas an opposite result appears for deuterium gas release. It is also clear that the total amount of deuterium released from D<sub>2</sub>O exposed sample is approximately 20 times more than the D<sub>2</sub> exposed sample. The experiment's obtained result suggests that, under D<sub>2</sub>O exposed condition and at 1175 K operating temperature, Y-doped barium-zirconate

might be preferable for electrochemical applications due to its higher hydrogen solubility.

### 4. CONCLUSIONS

In this study, hydrogen (deuterium) was dissolved in BaZr<sub>0.9</sub>Y<sub>0.1</sub>O<sub>3-α</sub> by the exposure of deuterium gas or heavy water vapor, and the amount of dissolved deuterium in the sample was measured by TDS method. It was observed that deuterium solubility is higher in the BZY sample under the D<sub>2</sub>O exposure condition and the release of deuterium was appeared at around 1175 K.

### 5. ACKNOWLEDGEMENTS

We would like to thank our laboratory members for their cordial support to operate the experimental instruments.

### 6. REFERENCES

- [1] H. Iwahara, Technological challenges in the application of proton conducting ceramics, *Solid State Ionics*. 77 (1995) 289–298. [https://doi.org/10.1016/0167-2738\(95\)00051-7](https://doi.org/10.1016/0167-2738(95)00051-7).
- [2] T. Norby, Mixed hydrogen ion–electronic conductors for hydrogen permeable membranes, *Solid State Ionics*. 136–137 (2000) 139–148. [https://doi.org/10.1016/S0167-2738\(00\)00300-3](https://doi.org/10.1016/S0167-2738(00)00300-3).
- [3] H. Iwahara, Prospect of hydrogen technology using proton-conducting ceramics, *Solid State Ionics*. 168 (2004) 299–310. <https://doi.org/10.1016/j.ssi.2003.03.001>.
- [4] X. Tan, J. Song, X. Meng, B. Meng, Preparation and characterization of BaCe<sub>0.95</sub>Tb<sub>0.05</sub>O<sub>3-α</sub> hollow fibre membranes for hydrogen permeation, *J. Eur. Ceram. Soc.* 32 (2012) 2351–2357. <https://doi.org/10.1016/j.jeurceramsoc.2012.03.004>.
- [5] IAEA, Safe handling of tritium Review of Data and Experience, in: IAEA (Ed.), *Tech. Reports Ser. No. 324*, International Atomic Energy Agency, Vienna, 1991: pp. 1–130.
- [6] M. Tanaka, Y. Asakura, T. Uda, Performance of the electrochemical hydrogen pump of a proton-conducting oxide for the tritium monitor, *Fusion Eng. Des.* 83 (2008) 1414–1418. <https://doi.org/10.1016/j.fusengdes.2008.06.038>.
- [7] M. Tanaka, T. Sugiyama, T. Ohshima, I. Yamamoto, Extraction of Hydrogen and Tritium Using High-Temperature Proton Conductor for Tritium Monitoring, *Fusion Sci. Technol.* 60 (2011) 1391–1394. <https://doi.org/10.13182/FST11-A12690>.
- [8] M. Tanaka, T. Sugiyama, Development of a Tritium Monitor Combined with an Electrochemical Tritium Pump Using a Proton Conducting Oxide, *Fusion Sci. Technol.* 67

- (2015) 600–603.  
<https://doi.org/10.13182/FST14-T89>.
- [9] Y. Kawamura, S. Konishi, M. Nishi, T. Kakuta, Transport Properties of Hydrogen Isotope Gas Mixture Through Ceramic Protonic Conductor, *Fusion Sci. Technol.* 41 (2002) 1035–1039. <https://doi.org/10.13182/FST02-A22741>.
- [10] Y. Kawamura, S. Konishi, M. Nishi, Extraction of Hydrogen from Water Vapor by Hydrogen Pump Using Ceramic Protonic Conductor, *Fusion Sci. Technol.* 45 (2004) 33–40. <https://doi.org/10.13182/FST04-A423>.
- [11] A. Ciampichetti, F.S. Nitti, A. Aiello, I. Ricapito, K. Liger, D. Demange, L. Sedano, C. Moreno, M. Succi, Conceptual design of Tritium Extraction System for the European HCPB Test Blanket Module, *Fusion Eng. Des.* 87 (2012) 620–624. <https://doi.org/10.1016/j.fusengdes.2012.01.047>.
- [12] H. IWAHARA, Study on Proton Conductive Solid Electrolyte-Recent Trends, *Electrochemistry.* 69 (2001) 788–793. <https://doi.org/10.5796/electrochemistry.69.788>.
- [13] O. Antoine, C. Hatchwell, G.C. Mather, A.J. McEvoy, Structure and Conductivity of a Yb-Doped SrCeO<sub>3</sub>-BaZrO<sub>3</sub> Solid Solution, *ECS Proc. Vol.* 2003–07 (2003) 379–387. <https://doi.org/10.1149/200307.0379PV>.
- [14] Y. Kawamura, T. Yamanishi, Tritium recovery from blanket sweep gas via ceramic proton conductor membrane, *Fusion Eng. Des.* 86 (2011) 2160–2163. <https://doi.org/10.1016/j.fusengdes.2010.12.003>.
- [15] R. Mukundan, E.L. Brosha, S.A. Birdsell, A.L. Costello, F.H. Garzon, R.S. Willms, Tritium Conductivity and Isotope Effect in Proton-Conducting Perovskites, *J. Electrochem. Soc.* 146 (2019) 2184–2187. <https://doi.org/10.1149/1.1391911>.
- [16] M.K. Hossain, K. Hashizume, S. Jo, K. Kawaguchi, Y. Hatano, Hydrogen Isotope Dissolution and Release Behavior of Rare Earth Oxides, *Fusion Sci. Technol.* 76 (2020) 553–566. <https://doi.org/10.1080/15361055.2020.1728173>.
- [17] W. Mao, T. Chikada, A. Suzuki, T. Terai, H. Matsuzaki, Hydrogen isotope dissolution, diffusion, and permeation in Er<sub>2</sub>O<sub>3</sub>, *J. Power Sources.* 303 (2016) 168–174. <https://doi.org/10.1016/j.jpowsour.2015.10.091>.
- [18] T. Chikada, T. Tanaka, K. Yuyama, Y. Uemura, S. Sakurada, H. Fujita, X.-C. Li, K. Isobe, T. Hayashi, Y. Oya, Crystallization and deuterium permeation behaviors of yttrium oxide coating prepared by metal organic decomposition, *Nucl. Mater. Energy.* 9 (2016) 529–534. <https://doi.org/10.1016/j.nme.2016.06.009>.
- [19] Y. Kawamura, K. Isobe, T. Yamanishi, Mass transfer process of hydrogen via ceramic proton conductor membrane of electrochemical hydrogen pump, *Fusion Eng. Des.* 82 (2007) 113–121. <https://doi.org/10.1016/j.fusengdes.2006.07.094>.
- [20] J. Melnik, J. Luo, K.T. Chuang, A.R. Sanger, Stability and Electric Conductivity of Barium Cerate Perovskites Co-Doped with Praseodymium, *Open Fuels Energy Sci. J.* 1 (2008) 7–10. <https://doi.org/10.2174/1876973X00801010007>.
- [21] K. Yamashita, T. Otsuka, K. Hashizume, Hydrogen solubility and diffusivity in a barium cerate protonic conductor using tritium imaging plate technique, *Solid State Ionics.* 275 (2015) 43–46. <https://doi.org/10.1016/j.ssi.2015.02.008>.
- [22] M.K. Hossain, H. Tamura, K. Hashizume, Visualization of hydrogen isotope distribution in yttrium and cobalt doped barium zirconates, *J. Nucl. Mater.* 538 (2020) 152207. <https://doi.org/10.1016/j.jnucmat.2020.152207>.
- [23] M.K. Hossain, K. Hashizume, Preparation and Characterization of Yttrium Doped Barium-Zirconates at High Temperature Sintering, in: *Int. Exch. Innov. Conf. Eng. Sci., Fukuoka, Japan, 2020:* pp. 70–72. <https://doi.org/10.15017/2552940>.
- [24] S. Maher, S.U. Syed, D.M. Hughes, J.R. Gibson, S. Taylor, Mapping the Stability Diagram of a Quadrupole Mass Spectrometer with a Static Transverse Magnetic Field Applied, *J. Am. Soc. Mass Spectrom.* 24 (2013) 1307–1314. <https://doi.org/10.1007/s13361-013-0654-5>.